

Spin-valley phase diagram of the two-dimensional metal-insulator transition

O. Gunawan, T. Gokmen, K. Vakili, M. Padmanabhan, E. P. De Poortere, and M. Shayegan
 Department of Electrical Engineering, Princeton University, Princeton, NJ 08544
 (dated: January 7, 2022)

Using symmetry breaking strain to tune the valley occupation of a two-dimensional (2D) electron system in an AlAs quantum well, together with an applied in-plane magnetic field to tune the spin polarization, we independently control the system's valley and spin degrees of freedom and map out a spin-valley phase diagram for the 2D metal-insulator transition. The insulating phase occurs in the quadrant where the system is both spin- and valley-polarized. This observation establishes the equivalent roles of spin and valley degrees of freedom in the 2D metal-insulator transition.

PACS numbers: 71.30.+h, 73.43.Qt, 73.50.Dn, 72.20.-i

The scaling theory of localization in two dimensions [1], which predicts an insulating phase for two-dimensional electron systems (2DESs) with arbitrarily weak disorder, was challenged by the observation of a metallic temperature dependence ($d\rho/dT > 0$) of the resistivity, ρ , in low-disorder Si metal-oxide-semiconductor field-effect transistors (Si MOSFETs) [2]. The associated metal-to-insulator transition (MIT) has subsequently become the subject of intense interest and controversy [3]. While behavior similar to that of Ref. [2] has now been reported for a wide variety of 2D carrier systems such as n-AlAs [4], n-GaAs [5], n-Si/SiGe [6, 7], p-GaAs [8, 9, 10], and p-Si/SiGe [11, 12], the origin of the metallic state and its transition into the insulating phase remain major puzzles in solid state physics.

Several experiments have demonstrated the important role of the spin degree of freedom in the MIT problem, either in systems with a strong spin-orbit interaction [10, 13, 14], or via the application of an external magnetic field to spin polarize the carriers [5, 16, 17, 18, 19]. The latter experiments have shown that a magnetic field applied parallel to the 2DES plane suppresses the metallic temperature dependence, ultimately driving the 2DES into the insulating regime as the 2DES is spin polarized. The relevance of multiple conduction-band valleys, on the other hand, is less known. Although it has been discussed theoretically that the occupation of multiple valleys may also be important [20, 21], there has been no direct experimental demonstration. Here we show that the electrons' valley degree of freedom indeed plays a crucial role, analogous to that of spin. We study a 2DES, confined to an AlAs quantum well, in which we can independently tune both the spin and valley degrees of freedom. By studying the temperature dependence of ρ at various degrees of spin and valley polarization, we map out the metal-insulator phase diagram in this system at a constant density. The 2DES exhibits a metallic behavior when either the valley or spin are left fully unpolarized, and a minimum amount of both spin and valley polarization is required to enter the insulating phase.

We performed experiments on 2DESs confined to modulation-doped, AlAs quantum wells of width 11 nm

and 15 nm [22]. In these systems, the electrons occupy two conduction-band valleys of AlAs centered at the edges of the Brillouin zone along the [100] and [010] directions. We denote these valleys as X and Y [Fig. 1(b)], according to the direction of their major axes. Each valley is characterized by a longitudinal $m_l = 1.1m_0$ and a transverse $m_t = 0.2m_0$ electron effective mass (m_0 is electron mass in vacuum). In our experiments we apply external strain in the plane of the sample to tune the populations of the X and Y valleys [23, 24, 25], and study the evolution of the 2DES as it becomes valley polarized. This is done by gluing the sample to one side of a stacked piezoelectric actuator with the sample's [100] crystal orientation aligned with the piezo's poling direction [Fig. 1(a)]. When a voltage bias V_{PZ} is applied to the piezo stack, it expands (shrinks) along [100] for $V_{PZ} > 0$ ($V_{PZ} < 0$) and shrinks (expands) in the [010] direction, thus inducing a symmetry breaking strain in the sample plane [26]. Such strain lifts the energy degeneracy between the X and Y valleys and electrons are transferred from one valley to another [Fig. 1(b)] while the total density stays constant. To measure the strain we use a metal-foil strain gauge glued to the piezo's back.

Our measurements were performed in a ^3He cryostat with a base temperature of 0.3 K. The piezo, with the glued sample, was mounted in this cryostat on a stage which could be tilted in-situ to control the direction of the magnetic field with respect to the sample plane. The stage allows us to apply a perpendicular magnetic field to characterize the sample via measuring its electron density and the population of the valleys, and then rotate the sample and apply an in-plane magnetic field (B_k) to induce Zeeman spin splitting and eventually spin-polarize the system. As schematically illustrated in Figs. 1(c) and (d), in our experiments B_k and strain play analogous roles as they allow us to tune the spin and valley polarization of the 2DES, respectively.

The strain vs B_k phase diagram of Fig. 1(g) captures our main observation. The origin in this figure, where both B_k and strain are equal to zero, represents the condition where the electrons are distributed equally between the X and Y valleys [27] and have zero spin polariza-

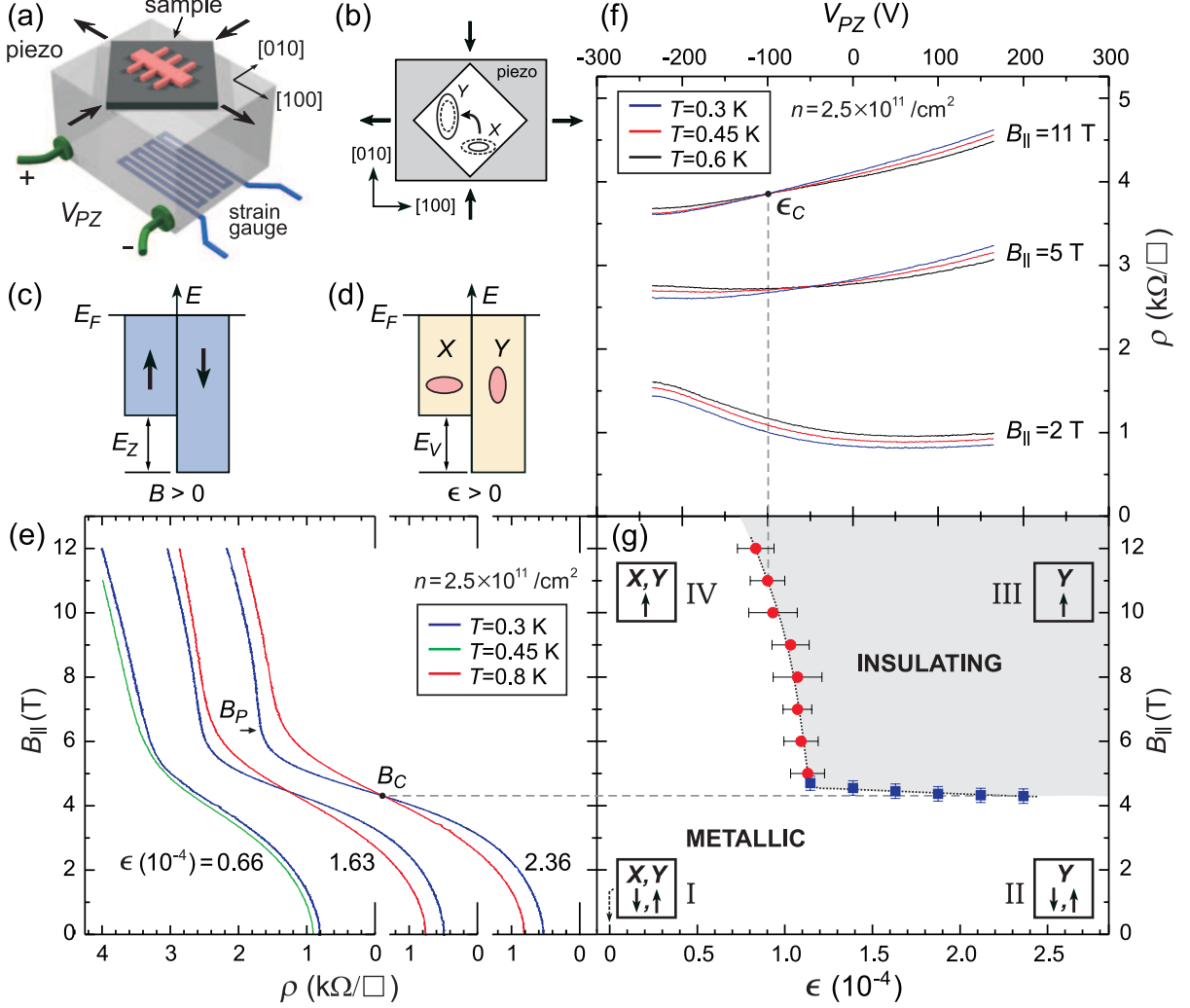


FIG. 1: (color online) (a) Schematic of the experimental set-up. The thick arrows indicate the situation where the sample is under tensile strain along [100] and compressive strain along [010]. (b) The corresponding electron transfer from the X to the Y valley. (c) and (d) Schematic diagrams showing the (Zeeman) spin and valley splittings (E_Z and E_V) with applied magnetic field or symmetry-breaking strain, respectively. (e) Magneto-resistance traces at various values of strain. (f) Piezo-resistance traces at different B_k . (g) The metal-insulator phase diagram spanning the four possible combinations of spin and valley occupation, indicated as insets at the four corners. The dotted arrow at $\epsilon = 0$ ($V_{PZ} = -285$ V) marks the piezo bias at which the valleys are equally occupied at $B_k = 0$. The squares and circles represent the critical points B_C and ϵ_C , deduced from temperature-dependent traces of (e) and (f), respectively. The dotted line, delineating the phase boundary, is a guide to the eye only. The sample is an 11 nm-wide AlAs quantum well with a density of $2.5 \times 10^{11} \text{ cm}^{-2}$ and mobility (at $\epsilon = 0$, $B_k = 0$, and $T = 0.3$ K) of $3.6 \text{ m}^2/\text{Vs}$.

tion. The opposite limit, where the 2DES is fully valley and spin polarized, is reached in the upper right corner of this diagram (quadrant III) for sufficiently large values of strain and B_k . In our experiments, we measure the temperature dependence of ρ as either of the two parameters ρ or B_k is kept constant and the other is swept to either spin or valley polarize the 2DES. Examples are presented in Fig. 1 (e) where ρ vs B_k traces are shown for two temperatures at three values of strain. For ϵ equal to 1.63×10^{-4} and 2.36×10^{-4} , the traces show that at low B_k the 2DES exhibits a metallic behavior ($d\rho/dT > 0$)

while above a critical field (B_C) the behavior turns insulating ($d\rho/dT < 0$). These critical fields are marked by blue squares in Fig. 1 (g). The traces at $\epsilon = 0.66 \times 10^{-4}$, on the other hand, show that the 2DES remains metallic in the entire range of applied B_k . In Fig. 1 (f), we show traces where B_k is kept fixed while strain is swept continuously. Here we see that at small values of B_k (e.g., 2 T) the sample exhibits a metallic behavior in the entire range of V_{PZ} , while at larger B_k , the metallic behavior at low V_{PZ} changes to insulating above a B_k -dependent critical ϵ_C . These ϵ_C are represented by red circles in

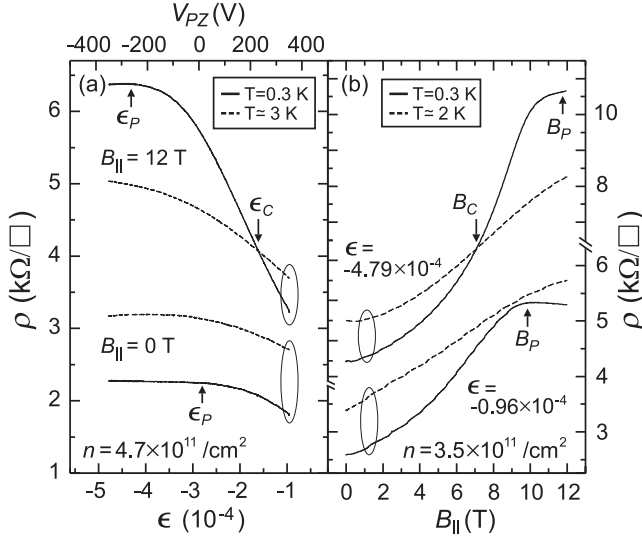


FIG. 2: Data for a 15 nm wide AlAs quantum well sample. (a) Piezo-resistance traces at $B_k = 0$ T, where the 2DES is spin unpolarized, and $B_k = 12$ T, where it is (almost) fully spin polarized. (b) Magneto-resistance traces at $\epsilon = -0.96 \times 10^{-4}$, where the 2DES is only slightly valley polarized, and $\epsilon = -4.79 \times 10^{-4}$ where it is fully valley polarized.

Fig. 1(g). The blue squares and red circles in Fig. 1(g) therefore define the boundary between the metallic and insulating phases of this 2DES. Figure 1(g) qualitatively establishes that the 2DES exhibits a metallic behavior unless there is a significant amount of spin and valley polarization (quadrant III).

Several features of the data in Figs. 1(e), (f), and (g) are noteworthy. The traces in Fig. 1(e), e.g., exhibit a large positive magneto-resistance, implying that, as the 2DES is made more spin polarized, its resistivity increases. This increase in ρ can be largely attributed to the loss of screening of the ionized impurities upon spin polarization of the 2DES [20, 28, 29]. We see a more subtle dependence of ρ on valley polarization [Fig. 1(f)]. At small B_k , when the spins are not polarized, ρ decreases with increasing valley polarization. This is because we are measuring ρ along [100] [Fig. 1(a)] and transferring electrons into the Y valley which has a smaller effective mass and therefore larger mobility along [100]. At sufficiently high B_k , when the electrons are nearly or fully spin polarized, however, the data of Fig. 1(f) show that ρ increases with strain even though electrons are transferred into the Y valley. This observation suggests that the screening of impurity potentials becomes weaker with valley polarization also, consistent with the theoretical calculations [20]. No matter what the cause of increasing ρ , experimentally it is clear from Figs. 1(e) and (f) that, at a fixed low temperature, ρ is largest in the insulating (III-IV) quadrant of Fig. 1(g) where the 2DES is most spin and valley polarized.

The above observations are further amplified by our

measurements on another AlAs sample (15 nm well-width), presented in Fig. 2. Here, in a separate cooldown and by placing the zero-strain condition at a large positive $V_{PZ} = 525$ V, we managed to reach large compressive strain values ($\epsilon < 0$) along the [100] direction and study the transport properties as the electrons are transferred into the X valley. Overall, the data are similar to those shown in Figs. 1(e) and (f): When the 2DES is spin or valley degenerate, its metallic behavior survives as it is made fully valley or spin polarized (bottom sets of traces in Fig. 2). On the other hand, when the 2DES is already significantly spin (or valley) polarized, its metallic behavior turns insulating as we valley (or spin) polarize it (top sets of traces in Fig. 2) [30]. Moreover, the piezo-resistance data, shown in Fig. 2(a), show that ρ increases as this charge transfer occurs even at $B_k = 0$. This is because both the expected loss of screening upon valley polarization, and the smaller mobility (along the current direction, i.e., [100]) of the X valley to which the electrons are transferred, lead to a rise in ρ . For completeness, in Fig. 2(b) we show the magneto-resistivity of the sample for different values of strain. The remarkable similarity of the data in Figs. 2(a) and (b) attests to the equivalent roles that the spin and valleys degrees of freedom play in the MIT problem.

The data of Figs. 1 and 2 reveal yet another important clue regarding the 2D MIT. In Figs. 1(e) and 2(b), we observe that the positive magneto-resistivity nearly saturates at high fields, beyond a field B_P , as marked in Figs. 1(e) and 2(b). The field B_P represents the magnetic field beyond which the 2DES is fully spin-polarized [16, 17, 18, 19, 28, 29, 31]. The fields B_C and B_P are close to each other but, as pointed out by Tutuc et al. [19], the fact that $B_C < B_P$ implies that the transition to the insulating phase occurs not at the full spin polarization field but rather when the population of minority spin electrons reaches below a threshold value. We find that the situation is similar for the onset of insulating behavior with valley polarization also: As seen in Fig. 2(a), the 2DES turns insulating at a critical strain (ϵ_C) which is smaller than the strain value at which the system becomes fully valley polarized (ϵ_P) [32]. The magnitude of spin and valley polarization needed to turn the 2DES insulating appears to depend on the system and density, but it is typically larger than about 50%.

Next, we note that the phase boundary denoted by the red circles in Fig. 1(g) is not vertical but shows a dependence on B_k . This simply reflects the fact that, thanks to the finite thickness of the electron layer, the energies of the X and Y valleys slightly shift with respect to each other as B_k increases. The shift comes about because the parallel field couples to the orbital motion of the electrons [33, 34] and changes the confinement energies of the X and Y valleys. Since X and Y valleys have anisotropic Fermi contours which are orthogonal to each other, the parallel field, which is applied along the major

axis of one valley (X) and perpendicular to the other (Y), couples differently to these valleys, causing a slight shift in their relative energies. We performed experiments in tilted magnetic fields and, by carefully monitoring the Landau levels for the X and Y valleys as a function of B_k , measured the shift between the energies of these valleys [35]. Correcting for this shift, the boundary between quadrants III and IV is nearly vertical.

In summary, a 2DES confined to an AlAs quantum well exhibits a metallic behavior when it is valley or spin degenerate. The system turns into an insulator when the valley and spins are both sufficiently polarized. The insulating phase has the largest resistivity at a given low temperature. The data establish experimentally the equivalence of the valley and spin degrees of freedom in the 2D MIT problem [36]. Based on studies of the role of spin, it has been suggested that temperature dependent scattering and screening are responsible for the apparent metallic behavior observed in 2D systems at finite temperatures [10, 13, 14, 18, 19, 20]. Our data presented here provide further credence to such an explanation.

We thank the NSF and ARO for support, and Y. P. Shkolnikov, E. Tutuc, and K. Lai for illuminating discussions.

-
- [1] E. Abraham, P. W. Anderson, D. C. Licciardello, and T. V. Ramakrishnan, *Phys. Rev. Lett.* **42**, 673 (1979).
- [2] S. V. Kravchenko, G. V. Kravchenko, J. E. Fumeaux, V. M. Pudalov, and M. D. Torio, *Phys. Rev. B* **50**, 8039 (1994).
- [3] See for example: E. Abraham, S. V. Kravchenko, and M. P. Sarachik, *Rev. Mod. Phys.* **73**, 251 (2001); S. V. Kravchenko and M. P. Sarachik, *Rep. Prog. Phys.* **67**, 1 (2004); S. DasSarma and E. H. Hwang, *Solid State Comm.* **135**, 579 (2005).
- [4] S. J. Papadakis and M. Shayegan, *Phys. Rev. B* **57**, R15 068 (1998).
- [5] Y. Hanein, D. Shahar, J. Yoon, C. C. Li, D. C. Tsui, and H. Shtrikman, *Phys. Rev. B* **58**, R13 338 (1998).
- [6] K. Lai, W. Pan, D. C. Tsui, and Y. H. Xie, *Appl. Phys. Lett.* **84**, 302 (2004); K. Lai, W. Pan, D. C. Tsui, S. A. Lyon, M. Muhlberger, and F. Schaefer, *Phys. Rev. B* **72**, R81 313 (2005).
- [7] T. Okamoto, M. Ooya, K. Hosoya, and S. Kawaji, *Phys. Rev. B* **69**, R41 202 (2004).
- [8] Y. Hanein, U. Meirav, D. Shahar, C. C. Li, D. C. Tsui, and H. Shtrikman, *Phys. Rev. Lett.* **80**, 1288 (1998).
- [9] M. Y. Simmons, A. R. Hamilton, M. Pepper, E. H. Linfield, P. D. Rose, D. A. Ritchie, A. K. Savchenko, and T. G. Richter, *Phys. Rev. Lett.* **80**, 1292 (1998).
- [10] S. S. Murzin, S. I. Dorozhkin, G. Landwehr, and A. C. Gossard, *JETP Lett.* **67**, 113 (1998).
- [11] J. Lam, M. D. Torio, D. Brown, and H. Lafontaine, *Phys. Rev. B* **56**, R12 741 (1997).
- [12] P. T. Coleridge, R. L. Williams, Y. Feng, and P. Zawadzki, *Phys. Rev. B* **56**, R12 764 (1997).
- [13] S. J. Papadakis, E. P. De Poortere, H. C. Manoharan, M. Shayegan, and R. Winkler, *Science* **283**, 2056 (1999).
- [14] Y. Yaish, O. Prus, E. Buchstab, S. Shapira, G. Ben Yoseph, U. Sivan, and A. Stem, *Phys. Rev. Lett.* **84**, 4954 (2000).
- [15] D. Simonian, S. V. Kravchenko, M. P. Sarachik, and V. M. Pudalov, *Phys. Rev. Lett.* **79**, 2304 (1997).
- [16] T. Okamoto, K. Hosoya, S. Kawaji, and A. Yagi, *Phys. Rev. Lett.* **82**, 3875 (1999).
- [17] J. Yoon, C. C. Li, D. Shahar, D. C. Tsui, and M. Shayegan, *Phys. Rev. Lett.* **84**, 4421 (2000).
- [18] S. J. Papadakis, E. P. De Poortere, M. Shayegan, and R. Winkler, *Phys. Rev. Lett.* **84**, 5592 (2000).
- [19] E. Tutuc, E. P. De Poortere, S. J. Papadakis, and M. Shayegan, *Phys. Rev. Lett.* **86**, 2858 (2001).
- [20] S. DasSarma and E. H. Hwang, *Phys. Rev. B* **72**, 205 303 (2005).
- [21] A. Punnoose and A. M. Finkelstein, *Science* **310**, 289 (2005).
- [22] E. P. De Poortere, Y. P. Shkolnikov, E. Tutuc, S. J. Papadakis, M. Shayegan, E. Palm, and T. Murphy, *Appl. Phys. Lett.* **80**, 1583 (2002) and references therein.
- [23] M. Shayegan, K. Karrai, Y. P. Shkolnikov, K. Vakili, E. P. De Poortere, and S. M. Anus, *Appl. Phys. Lett.* **83**, 5235 (2003).
- [24] Y. P. Shkolnikov, K. Vakili, E. P. De Poortere, and M. Shayegan, *Appl. Phys. Lett.* **85**, 3766 (2004).
- [25] O. Gunawan, Y. P. Shkolnikov, K. Vakili, T. Gokmen, E. P. De Poortere, and M. Shayegan, *cond-mat/0605692*. As detailed in this reference, the valley splitting E_V is equal to the product of strain and a constant (deformation potential) which can depend on the 2DES density.
- [26] Here we define strain as $\epsilon = \frac{\Delta l_{[100]}}{l_{[100]}} - \frac{\Delta l_{[010]}}{l_{[010]}}$, where $\frac{\Delta l_{[100]}}{l_{[100]}}$ and $\frac{\Delta l_{[010]}}{l_{[010]}}$ are the fractional changes in sample's size along the [100] and [010] directions.
- [27] Thanks to finite residual stress during the cooling of the sample and the piezo, we need a finite, cooldown-dependent V_{PZ} to attain the zero-strain condition in our experiments. We determine this V_{PZ} from our detailed Shubnikov-de Haas and coincidence measurements as detailed in Ref. [25]. For the data of Fig. 1, we determined the zero-strain condition to be at $V_{PZ} = 285$ V, and have marked it in Fig. 1(g) by a dotted arrow.
- [28] V. T. Dolgoplov and A. Gold, *JETP Lett.* **71**, 27 (2000).
- [29] I. F. Herbut, *Phys. Rev. B* **63**, 113 102 (2001).
- [30] From our measurements in the low-temperature regime ($0.3 < T < 0.8$ K), we also determined the boundaries between the metallic and insulating phases for the 15 nm quantum well at a density of $4.7 \times 10^{11} \text{ cm}^{-2}$: A suspected for this higher density, the boundary is pushed to larger values of B_k (10 T) and j_j (2×10^{-4}).
- [31] Y. P. Shkolnikov, K. Vakili, E. P. De Poortere, and M. Shayegan, *Phys. Rev. Lett.* **92**, 246 804 (2004).
- [32] We experimentally determine ϵ_P from the saturation of the piezo-resistance, as observed in Fig. 2(a), as well as careful measurements of the Shubnikov-de Haas oscillations and "valley-coincidence" measurements, some of which are described in Ref. [25].
- [33] S. DasSarma and E. H. Hwang, *Phys. Rev. Lett.* **84**, 5596 (2000).
- [34] E. Tutuc, S. Melinte, E. P. De Poortere, M. Shayegan, and R. Winkler, *Phys. Rev. B* **67**, R241 309 (2003).
- [35] T. Gokmen, O. Gunawan, Y. Shkolnikov, K. Vakili, E. P. De Poortere, and M. Shayegan, unpublished.
- [36] The equivalent roles of spin and valley degrees of freedom

can also be seen in the equally enhanced spin and valley susceptibilities in AAs 2DESs [25].